Heliyon 9 (2023) e17236

Contents lists available at ScienceDirect

Heliyon

journal homepage: www.cell.com/heliyon

Kinetics of maize cob and bean straw pyrolysis and combustion

David K. Okot [a,b,*], Paul E. Bilsborrow [c], Anh N. Phan [a], David A.C. Manning [c]

[a] School of Engineering, Chemical Engineering, Newcastle University, UK
[b] Department of Physics, Faculty of Science, Mbarara University of Science and Technology, Uganda
[c] School of Natural and Environmental Sciences, Newcastle University, UK

ARTICLE INFO

Keywords:
Maize cob
Bean straw
Kinetic study
Activation energy
Pyrolysis and combustion

ABSTRACT

Kinetic studies are important for the design and optimisation of thermochemical processes. This study involved analysis of the pyrolysis and combustion behaviour of the agricultural residues (bean straw and maize cob) by non-isothermal thermogravimetric analysis. Increasing the heating rate from 10 to 40 K min^{-1} during both combustion and pyrolysis increased the degradation rate of both feedstocks and the gaseous yields of H_2O, CO and CO_2. The activation energies determined by the Flynn-Wall-Ozawa and Kissinger-Akahira-Sunose methods varied which reveals that the pyrolysis and combustion of these agricultural residues are complex processes involving multiple reactions. The average activation energy of maize cob and bean straw were 214.15 and 252.09 kJ mol^{-1} for pyrolysis and 202.26 and 165.64 kJ mol^{-1} for combustion, respectively. The order of reaction ranged between 9.0-10.3 and 6.3–13.3 for both feedstocks in combustion and inert environments, respectively. Modelled data is important to enable the optimisation of reactor design for pyrolysis and combustion for energy generation from agricultural residues.

1. Introduction

Biomass is a CO_2 neutral abundant energy source which accounts for about 10% of global primary energy consumption with further expansion predicted in the future [1]. Maize and bean are commonly cultivated crops globally, thereby generating large volumes of agricultural residues [2] with the potential for energy generation. The global productions of bean and maize are estimated to be 28.9 [3] and 1147 million tonnes [4] respectively. Combustion is the most widely used technology globally [5], while pyrolysis is gaining interest because of its potential to produce solid (char), liquid (bio-oil), and gaseous components [6–8] with the potential for a wide range of potential uses e.g. heat, electricity, transport fuel, hydrogen production, energy storage etc. Kinetic studies provide vital information in designing and modelling of combustion/pyrolysis and gasification systems as pyrolysis is an intermediate step providing a correlation between reaction temperature (T), conversion rate (α) and reaction rate constant (k) [9]. Kinetic studies can also help in explaining how different processes in a pyrolizer/gasifier affect product yields and composition [10].

Thermogravimetric analysis (TGA) is the most common technique to study the thermal behaviour of materials and to derive kinetic parameters such as activation energy and order of reaction. The methods used in analysing kinetic parameters are categorised as model fitting and model free. Model fitting involves fitting different models to the data and the model with the best statistical fit is then chosen for determination of the kinetic parameters. Model fitting methods require only a single TGA measurement for a complete kinetic study. However, their inability to uniquely determine the kinetic model is a challenge unlike for model-free methods where

* Corresponding author. School of Engineering, Newcastle University, UK.
E-mail address: okotkilama@must.ac.ug (D.K. Okot).

https://doi.org/10.1016/j.heliyon.2023.e17236
Received 6 August 2022; Received in revised form 8 June 2023; Accepted 12 June 2023
Available online 13 June 2023

Table 1
Properties of bean straw and maize cob feedstocks (values in the bracket are standard deviation for **n = 3**).

Property	Maize cob	Bean straw
Proximate analysis (dry basis)		
Ash (% wt)	3.0 (±0.5)	6.2 (±0.7)
Volatile (% wt)	80.7 (±0.7)	72.7 (±4.9)
Fixed carbon[a] (% wt)	16.3 (±0.9)	21.1 (±4.9)
Ultimate analysis (dry and ash free)		
C (%)	46.6 (±1.9)	45.0 (±2.6)
H (%)	7.7 (±1.2)	5.8 (±0.0)
N (%)	2.1 (±0.6)	2.0 (±1.0)
O[a] (%)	43.6 (±2.3)	47.2 (±2.8)
High heating value (HHV) (MJ kg^{-1})	18.9 (±0.1)	17.3 (±1.0)

[a] By the difference.

kinetic parameters are determined without pre-assumption of a model and the errors associated with wrong presumption of the model can be eliminated [11]. Furthermore, the model free method is flexible (accommodating changes in reaction mechanism) and uses multiple heating rates which minimises mass transfer limitations [12]. Model free methods are the most common method which have been used to study the kinetics of biomass materials such as microalgae [13], cardoon [14], Para grass (*Urochloa mutica*) [15], smooth cordgrass (*Spartina alterniflora*) [16], coffee husk [17] and wood based feedstocks (*Pinus elliottii*, *Eucalyptus grandis*, *Mezilaurus itauba* and *Dipteryx odorata*) [18]. Iso-conversional (model free) methods are used to determine kinetic parameters without pre-assumption of a model whereby the error associated with wrong presumption of the model can be eliminated [11]. They are based on the assumption that the reaction rate of any conversion is only dependent on temperature [19]. However, studies in the literature show significant variations in kinetic parameters associated with different feedstocks, together with the atmosphere and analytical approaches used [15,16,19–25]. Gupta and Mondal [26], studied the kinetics of maize cob pyrolysis using Friedman, FWO, KAS and Starink methods and reported that the average activation energies were 197.63, 186.06, 185.39 and 185.80 kJ mol^{-1} respectively. While Castiblanco et al. [27], assessed the effect of CaO and $CaCO_3$ on the kinetic parameters of maize cob pyrolysis and reported that addition of CaO or $CaCO_3$ increased the activation energy from 58.35 to 69.33 and 66.07 kJ mol^{-1}, respectively. Although the kinetics of maize cob pyrolysis have been studied previously, combustion and the evolving gases during the pyrolysis process have not been studied. Furthermore, to our knowledge there are no kinetic studies in the literature on the pyrolysis and combustion of bean straw. This study focussed on analysing the combustion and pyrolysis behaviour of corn cob and bean straw with the development of kinetic models from model fitting (i.e. universal integral approach) and model-free methods i.e., Flynn-Wall-Ozawa (FWO) and Kissinger-Akahira-Sunose (KAS) in combination.

2. Materials and methods

Bean straw obtained from Nafferton Farm (a research/commercial farm owned and managed by Newcastle University; 54°59′07.1″N, 1°53′59.4″W), was part of an organic crop rotation left as residue in the field to dry before being collected and stored under cool/dry conditions. Maize cobs were kindly provided by Barfoots of Botley Ltd, UK (https://www.barfoots.com). Maize (supersweet varieties) was harvested at Stage R3 (milk stage) of maturity in a range of countries (Senegal, Morocco, United States of America, South Africa, Greece, Germany, United Kingdom, France and Spain) and stored at 273–278 K for 1–25 days. Proximate analysis of maize cob and bean straw (Table 1) was conducted following the BS1016-6 standard. Ultimate analysis (i.e., CHN) was carried out using a Carlo Erba 1108 Elemental Analyser. High heating value (HHV) was determined using a CAL2K ECO bomb calorimeter.

2.1. Thermogravimetric analysis (TGA)

Prior to the TGA experiments, raw/dried maize cob and bean straw samples were ground to a particle size <250 μm to minimise mass and heat transfer limitations [14]. About 10 mg of sample was placed in a Netzsch Jupiter STA 449C TG-DSC system connected to a Netzsch Aeolos 403C quadrupole mass spectrometer (QMS). The system was heated from 298 to 1273 K at a heating rate of 10, 20, 30 and 40 K min^{-1} in either helium or a mixture of 20% oxygen +80% helium by volume (referred to as air subsequently) at a flow rate of 30 ml min^{-1}. These heating rates were low enough to favour efficient homogenous decomposition and minimise mass and heat transfer effects. High heating rate produces a large temperature gradient within particles, thereby affecting the kinetic parameters [28]. The QMS was operated in full scan mode over the range m/z 10–300 and mass spectrometric data were acquired and processed using Quadstar version 7.x.

2.2. Kinetic modelling

The iso-conventional Kissinger-Akahira-Sunose (KAS) and Flynn-Wall-Ozawa (FWO) methods were used to determine activation energies as they do not require any knowledge of the reaction mechanism [11,29]. The methods assume that the reaction rate is independent of heating rate [14]. Data obtained from TGA experiments was used to determine conversion, α (a fraction of the material

decomposed in time t [24]). The conversions outside the range 0.1–0.8 were not considered in the KAS and FWO plots while determining the activation energy due to low correlation values [22]. Furthermore, the first 10% conversion is affected by evaporation of water while the last 20% is not considered, because the mass loss is negligible. The pre-exponential factor and the reaction order were determined following the Universal Integral method [13]. Due to the complexity of the pyrolysis and combustion processes and the composition of the feedstocks, a simple first order reaction scheme (Equation (1)) with an associated kinetic model was adopted [30].

$$A_{(s)} \xrightarrow{k} bB_{(s)} + (1-b)C_{(g)} \tag{1}$$

where A(s) is the initial solid reactive, B(s) is the solid residue, b is the production coefficient of B(s), C(g) is the volatile matter formed and k is the reaction rate constant defined as;

$$k(T) = Aexp\left(-\frac{E}{RT}\right) \tag{2}$$

where A (min^{-1}) is pre-exponential factor, R is the universal gas constant (8.314 J K^{-1} mol^{-1}), E (kJ mol^{-1}) is the activation energy and T (K) is the temperature.

The thermal degradation of a material is defined from the TGA data in terms of conversion, α (a fraction of the material decomposed in time t) that is obtained from Equation (3) [24].

$$\alpha = \frac{m_o - m_t}{m_o - m_f} \tag{3}$$

where m_o = initial mass of feedstock, m_t = mass of feedstock at time t and m_f=final mass.

The rate of thermal degradation/conversion of biomass, defined as reaction rate is given by Equation (4) [13,31].

$$\frac{d\alpha}{dt} = k(T)f(\alpha) \tag{4}$$

where: $f(\alpha)$ is a differential reaction model, T is the sample temperature and k(T) is the reaction rate constant as a function of temperature (Arrhenius equation) as described by Equation (2). From Equations (2) and (4), the reaction rate can be expressed as:

$$\frac{d\alpha}{dt} = Aexp\left(-\frac{E}{RT}\right)f(\alpha) \tag{5}$$

For the non-isothermal process, temperature changes with time at a constant heating rate [23].

$$\beta = \frac{dT}{d\alpha}.\frac{d\alpha}{dt}. \tag{6}$$

Combining equations (5) and (6) gives

$$\frac{d\alpha}{dT} = \frac{A}{\beta}exp\left(-\frac{E}{RT}\right)f(\alpha) \tag{7}$$

Equation (7) is the differential form of the kinetic equation and consequently, the integral form is

$$g(\alpha) = \int_0^{\alpha} \frac{d\alpha}{f(\alpha)} = \int_{T_o}^{T} \frac{A}{\beta} e^{\left(\frac{-E}{RT}\right)} dT = \frac{AE}{\beta R}\int_x^{x_o} x^{-2}e^{-x}dx = \frac{AE}{\beta R}P(x) \tag{8}$$

where $g(\alpha)$: the integral reaction model, T_o and T are the temperatures at the beginning and end of the reaction respectively, $x : \frac{E}{RT}$ and P(x) is a temperature integral with no exact analytical solution. Equations (7) and (8) are used in the determination of the kinetic parameters by either isoconversional or model-based methods. Equation (8) is solved by use of approximation. The difference between the iso-conversional methods is therefore based on the type of approximation used in solving Equation (8) [14].

2.2.1. *Kissinger-Akahira-Sunose (KAS)*

Kissinger-Akahira-Sunose (KAS), uses the approximation given by Equation (9) [14].

$$P(x) = x^{-2}e^{-x} \tag{9}$$

which is substituted in Equation (8) to give Equation (10).

$$In\left(\frac{\beta}{T^2}\right) = In\left(\frac{AE}{Rg(\alpha)}\right) - \frac{E}{RT} \tag{10}$$

A plot of $In\left(\frac{\beta}{T^2}\right)$ against $\frac{1}{T}$ for each conversion ratio produces a straight-line graph whose slope is used to obtain the activation energy.

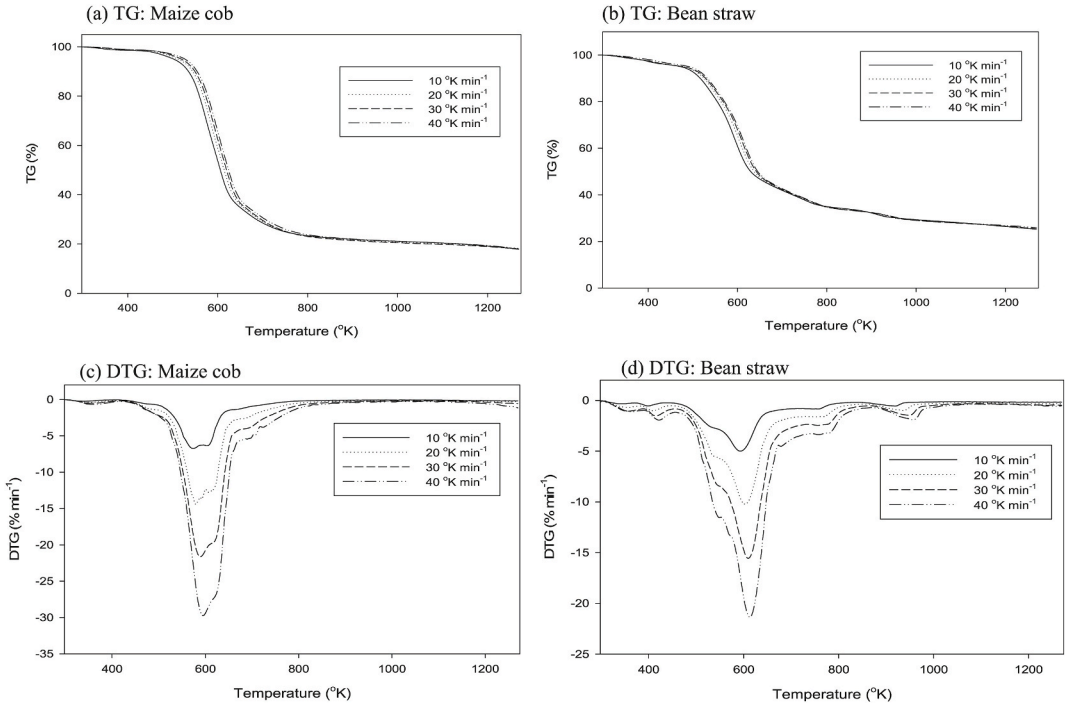

Fig. 1. Thermogravimetric (TG) of (a) maize cob and (b) bean straw, and differential thermogravimetric (DTG) curves of (c) maize cob and (d) bean straw in He at heating rates of 10, 20, 30 and 40 °C min^{-1}.

2.2.2. *Flynn-Wall-Ozawa (FWO)*

Flynn-Wall-Ozawa (FWO), uses Doyle's approximation:

$$log(p(x)) \approx -2.315 + 0.457x \tag{11}$$

Combining Equations (8) and (11) gives Equation (12), the FWO model.

$$log\,\beta = log\left(\frac{AE}{Rg(\alpha)}\right) - 2.315 - 0.457\frac{E}{RT} \tag{12}$$

The activation energy is obtained from the slope of the plot of $log\,\beta$ against $\frac{1}{T}$.

2.2.3. *Universal integral*

Rearranging Equation (5) and integrating both sides

$$g(\alpha) = A\,exp\left(\frac{-E}{RT}\right)t \tag{13}$$

For the non-isothermal process, temperature, T of experiment at time, t is determined by Equation (14) [23].

$$T = \beta t + T_o \tag{14}$$

Substituting for t from Equation (14) in Equation (13),

$$g(\alpha) = \frac{A}{\beta}(T - T_0)exp\left(-\frac{E}{RT}\right) \tag{15}$$

Rearranging Equation (15) and introducing natural log (ln) on both sides, gives Equation (16).

$$In\left[\frac{g(\alpha)}{T - T_0}\right] = In\left[\frac{A}{\beta}\right] - \frac{E}{RT} \tag{16}$$

A plot of $In\left[\frac{g(\alpha)}{T-T_0}\right]$ against $\frac{1}{T}$ gives a straight line whose gradient is $-\frac{E}{R}$, from which the activation energy is calculated and compared with the value obtained from FWO and KAS. The intercept is $In\left[\frac{A}{\beta}\right]$ from which the pre-exponential factor A is calculated [13]. The order of reaction n is obtained from the integral reaction model $g(\alpha)$.

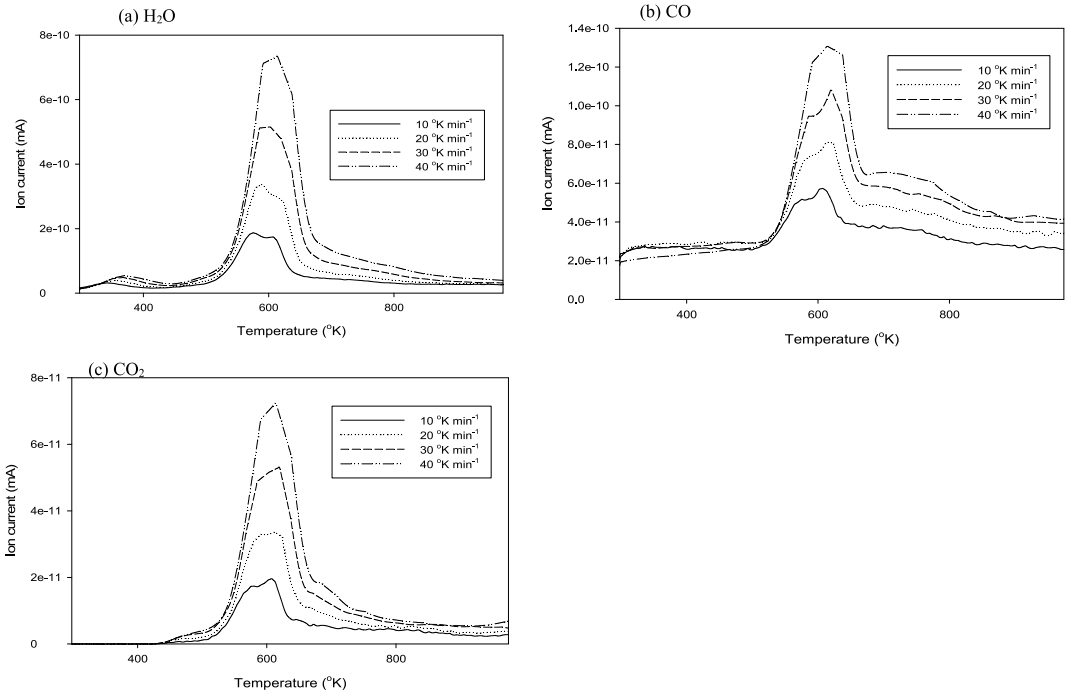

Fig. 2. Effect of heating rate on (a) H_2O, (b) CO and (c) CO_2 release from maize cob in an inert environment.

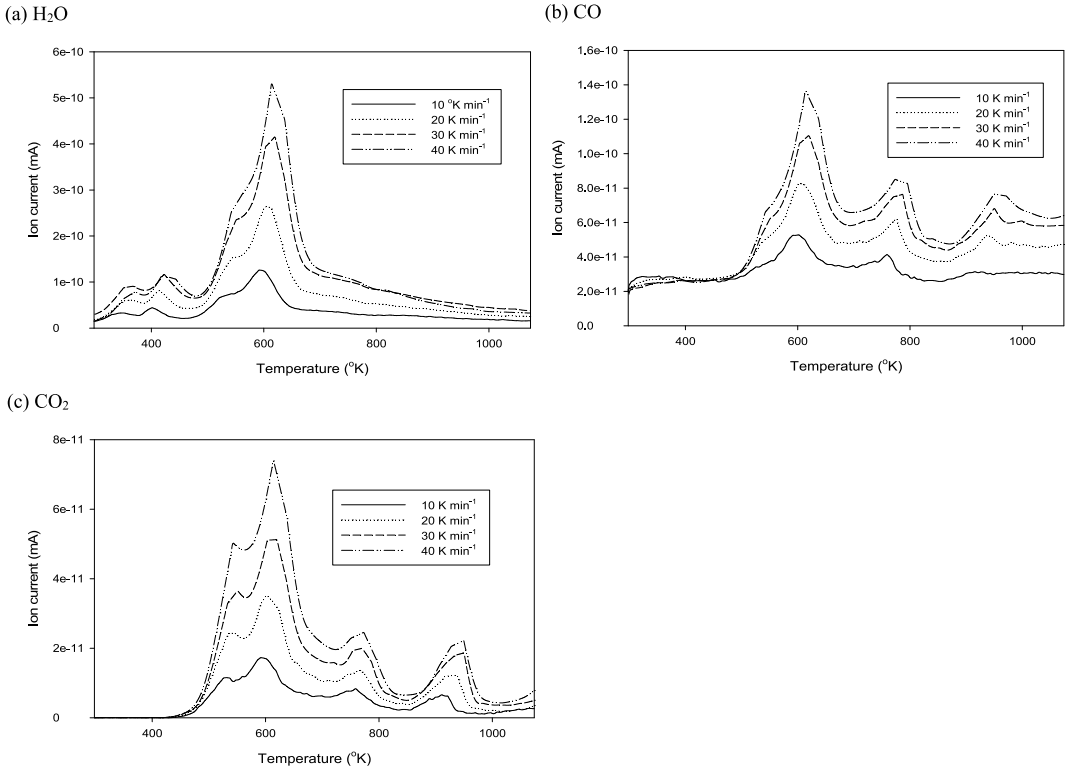

Fig. 3. Effect of heating rate on (a) H_2O, (b) CO and (c) CO_2 release from bean straw in an inert environment.

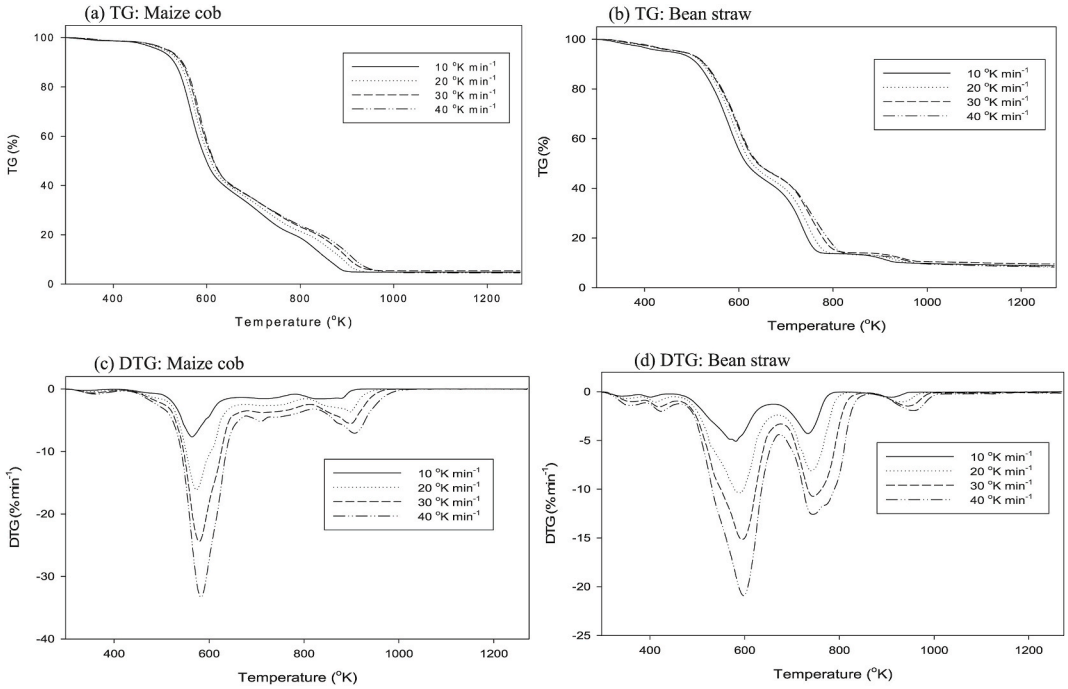

Fig. 4. A comparison of thermogravimetric (TG) of (a) maize cob and (b) bean straw, and differential thermogravimetric (DTG) curves of (c) maize cob and (d) bean straw in air.

3. Results and discussion

3.1. Pyrolysis of maize cob and bean straw (TGA in He, an inert environment)

Maize cob and bean straw showed a three-stage decomposition in helium (He) (Fig. 1a and b) i.e. moisture release at temperatures below 473 K (Stage I); decomposition of hemicellulose and cellulose together with partial decomposition of lignin 473-682 K for maize cob and 473–738 K for bean straw (Stage II); and lignin/primary char decomposition between 682 and 1273 K for maize cob and 738–1273 K for bean straw (Stage III). Char decomposition involved C–H and C–O bond cleavage, forming a carbon rich solid [32].

The highest rate of weight loss was attained during Stage II (Fig. 1) due to the release of volatiles, with residual weights of 18% and 25–26% for maize cob and bean straw respectively at the end of this stage. The rate of weight loss was greater with increasing heating rate from 10 to 40 K min^{-1} (Fig. 1c and d). The rate of weight loss became higher and broader with increasing heating rate because components in the biomass degrade simultaneously at high heating rate thereby causing an overlap between the peaks [16]. The heating of biomass particles at a low heating rate occurs gradually leading to more effective heat transfer to the material bed and between the biomass particles [33]. Heat transfer is not effective at higher heating rate (meaning, more time or a higher thermal gradient is required to complete the thermal degradation [33]), therefore the minimum heat required for cracking feedstocks to release volatiles is reached later at higher temperatures [24,34], causing the simultaneous decomposition of the biomass components. Increasing heating rate generates a large temperature gradient across the biomass particles due to low thermal conductivity of the material [35]. The peak between 923 and 965 K (Fig. 1d) could be due to the decomposition of a thermally stable organic carbon (char) not seen in the other sample, consistent with the evolved gas data (see later).

The effect of heating rate on the decomposition rate was also reflected in the peak yields of, H_2O (Figs. 2a and 3a), CO (Figs. 2b and 3b) and CO_2 (Figs. 2c and 3c) which corresponded to the peak DTG temperature. The H_2O peak at a temperature <473 K corresponds to the release of cellular water and external water held by surface tension [36]. The peak CO_2, CO and H_2O yields at temperatures of 473–682 K for maize cob and 473–738 K for bean straw are due to condensation and, decomposition such as decarbonylation and decarboxylation. Decomposition forms unstable compounds such as carbonyl and carboxyl groups which then undergo dehydration, fragmentation and secondary reactions to form CO_2, CO and H_2O [37]. The trends of the TG and DTG curves agree well with those for other biomass materials such as cardoon leaves and stem [14], para grass [15] and smooth cordgrass [16].

3.2. Combustion of maize cob and bean straw (TGA in 80%He 20% O)

At a temperature >473 K, a significant reduction in mass was observed up to 676 K for bean straw and 686 K for maize cob (Fig. 4a and b). The highest rate of weight loss was due to the release of volatiles which were subsequently oxidised. The slower rate of oxidation of partially decomposed lignin and char occurred at a temperature range of 676–1273 K for bean straw and 686–1273 K for

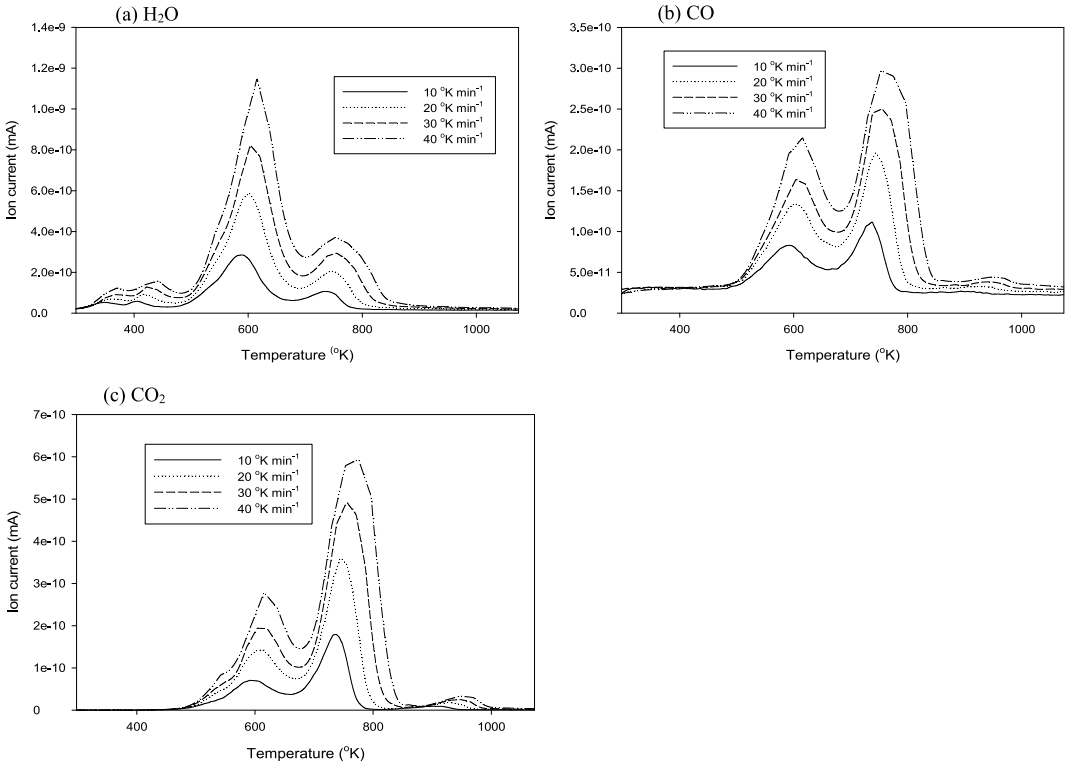

Fig. 5. Effect of heating rate on the yield of, (a) H_2O, (b) CO and (c) CO_2 following the combustion of bean straw in air.

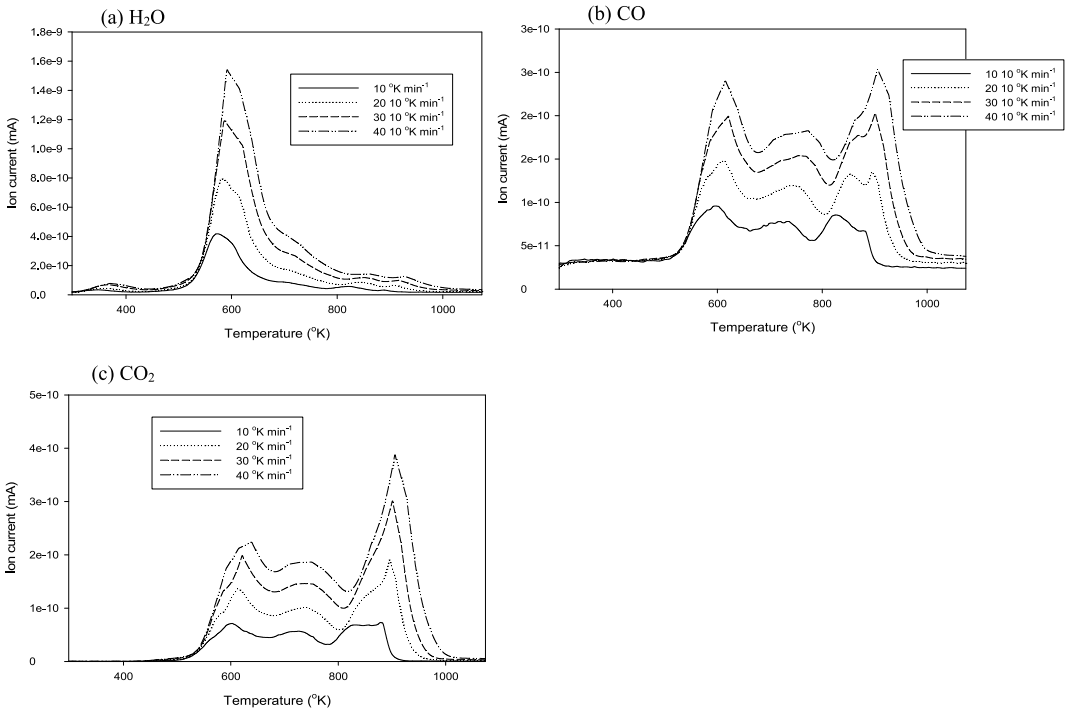

Fig. 6. Effect of heating rate on the yield of, (a) H_2O, (b) CO and (c) CO_2 following the combustion of maize cob in air.

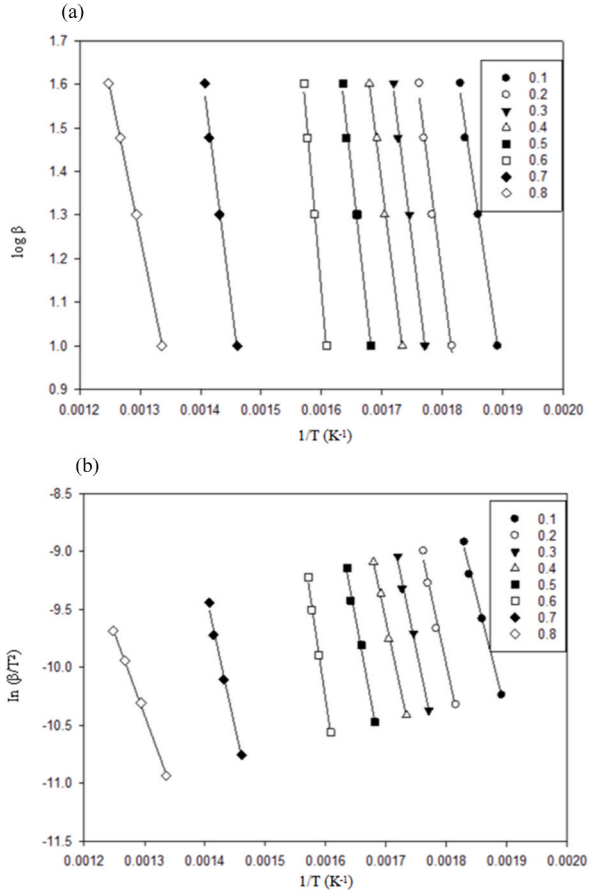

Fig. 7. Kinetic plots for maize cob using (a) Flynn-Wall-Ozawa and (b) Kissinger-Akahira-Sunose in air.

maize cob. This reaction is diffusion limited, as oxygen needs to diffuse into the particle or react at the surface of the char particle. The residual ash content of the feedstock was around 5% for maize cob and 8–9% for bean straw. The TG and DTG profiles were similar to those obtained from the combustion of other biomass feedstocks i.e. olive prunings, cotton residue, cardoon, olive kernels and peach kernels [38], empty fruit bunches and palm kernel shell [39]. As with pyrolysis, CO_2, CO and H_2O were detected in the gaseous product (Figs. 5 and 6). The impact of varying heating rate on the TGA/DTG (Fig. 4a–d) and gas profiles (Fig. 5a–c and 6(a–c)) from combustion of both feedstocks were identical to those observed following pyrolysis. The H_2O peaks at a temperature <473 K (Fig. 5a) were due to the release of absorbed moisture. The H_2O yields peaked between 473 and 676 K for bean straw and 473–686 K for maize cob (Fig. 6 a) which were likely attributed to combustion of oxygen containing functional groups, most especially hydroxyl groups as suggested by Li et al. [36]. Meanwhile, the H_2O produced at temperatures >676 K for bean straw and 686 K for maize cob were likely due to the combustion of H_2 (produced from dehydrogenation) and other volatiles i.e. CH_4 and other hydrocarbons/oxygenated compounds (produced from demethylation). The CO and CO_2 peaks between 473 and 676 K for bean straw (Fig. 5b and c) and 473–686 K for maize cob (Fig. 6b and c) were due to decomposition of carboxyl and carbonyl groups. Between 676 and 1073 K for bean straw and 686–1073 K for maize cob, the CO and CO_2 yields corresponded to the combustion of volatiles and the carbon rich solid residue [40] and Boudouard reaction i.e. $C + CO_2 \leftrightarrow 2CO$.

3.3. Kinetic parameters

The regression lines for FWO and KAS were parallel (Figs. 7 and 8) with high correlation coefficients ($R^2 > 0.94$) (Tables 1 and 2), thereby suggesting that the order and mechanism of thermal degradation reactions are similar [22] with a high degree of accuracy of the results [41]. Similar regression plots were also reported for melon seed husk [22]. The activation energies calculated from both KAS and FWO were conversion dependent, indicating that pyrolysis and combustion of bean straw and maize cob involve multiple reactions such as thermal cracking, condensation and depolymerisation (Tables 2 and 3). Such variations in activation energies following thermal conversion were also reported for soybean straw [42], poplar wood [11] and smooth cordgrass [16]. The average activation energies obtained by KAS and FWO were 213–215 kJ mol $^{-1}$ for maize cob and 250–254 kJ mol $^{-1}$ for bean straw in an inert environment but were higher than the 202 kJ mol $^{-1}$ for maize cob and 165–167 kJ mol $^{-1}$ for bean straw in air (Tables 2 and 3). The difference in activation energies obtained from the two methods was negligible, likely due to the distinctive linear approximation to

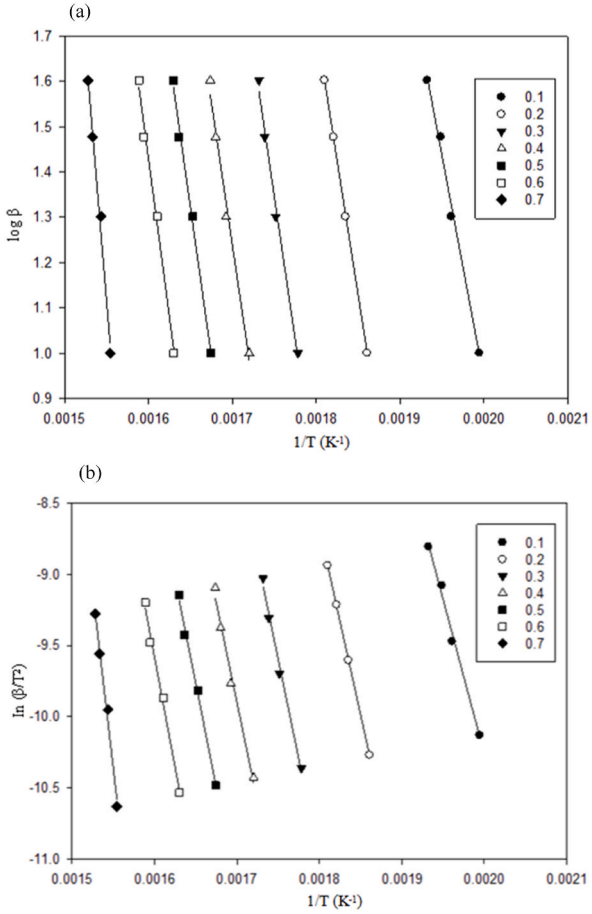

Fig. 8. Kinetic plots for bean straw using (a) Flynn-Wall-Ozawa and (b) Kissinger-Akahira-Sunose in He.

Table 2
Activation energy (E) and coefficient of determination (R^2) of maize cob and bean straw in an inert atmosphere (He) using both Flynn-Wall-Ozawa (FWO) and Kissinger-Akahira-Sunose (KAS).

Conversion	Maize cob				Bean straw			
	E (kJ mol^{-1})		R^2		E (kJ mol^{-1})		R^2	
	FWO	KAS	FWO	KAS	FWO	KAS	FWO	KAS
0.1	153.56	152.72	0.9915	0.9845	179.59	180.4	0.993	0.9924
0.2	192.35	192.93	0.9976	0.9974	215.63	217.69	0.9999	0.9999
0.3	202.05	202.89	0.9976	0.9974	230.36	232.78	0.9929	0.9923
0.4	210.55	211.63	0.9976	0.9973	229.89	231.96	0.9877	0.9867
0.5	219.22	220.55	0.9976	0.9973	239.99	242.30	0.9927	0.9921
0.6	229.58	231.19	0.9976	0.9973	252.84	255.56	0.9927	0.9920
0.7	240.15	242.10	0.9975	0.9973	405.09	415.20	0.9899	0.9894
0.8	257.52	267.43	0.9425	0.9587	–	–	–	–
Average	213.12	215.18			250.48	253.70		

the temperature integral [43]. The high level of similarity confirms the predictive power of KAS and FWO. As shown in Tables 2 and 3, a lower activation energy in air than He is due to heat generated from exothermic oxidation/combustion reactions in air and also indicating that both feedstocks had lower porosity for He than for air. The higher activation energy in He indicates that combustion is easier than pyrolysis from a reactivity viewpoint. Similar results were reported for tobacco waste [44]. The activation energy of bean straw in air was much lower than in helium which could be due to the higher oxygen content of bean straw (47.2%) as the organically bound oxygen in the feedstock would provide some of the oxygen required for combustion [45]. However, the activation energy of bean straw in He was higher than that of maize cob likely due to the higher volatile content in maize cob where more energy is required to decompose the fixed carbon in bean straw. Therefore, these results suggest that bean straw has higher thermal resistance to degradation than maize cob in an inert environment i.e. He which is likely due to the much higher lignin content of bean straw (10.2%

Table 3
Activation energy (E) and coefficient of determination (R^2) of maize cob and bean straw in air (80% He + 20% O_2) using Flynn-Wall-Ozawa (FWO) and Kissinger-Akahira-Sunose (KAS).

Conversion	Maize cob				Bean straw			
	E (kJ mol^{-1})		R^2		E (kJ mol^{-1})		R^2	
	FWO	KAS	FWO	KAS	FWO	KAS	FWO	KAS
0.1	171.57	171.49	0.9937	0.9930	165.24	165.19	0.9317	0.9251
0.2	197.68	198.60	0.9850	0.9836	188.05	188.59	0.9893	0.9883
0.3	206.44	207.57	0.9938	0.9932	182.10	181.97	0.9919	0.9911
0.4	201.63	202.30	0.9961	0.9957	175.10	174.29	0.9978	0.9976
0.5	228.63	230.41	0.9938	0.9932	169.63	168.18	0.9958	0.9952
0.6	287.10	291.46	0.9952	0.9949	120.16	115.37	0.9883	0.9859
0.7	199.81	198.52	0.9920	0.9911	166.42	163.09	0.9932	0.9922
0.8	124.64	118.21	0.9992	0.9989	165.36	161.49	0.9883	0.9864
Average	202.19	202.32			166.51	164.77		

Table 4
Reaction order (n) and pre-exponential factor (A) following pyrolysis in air (80% He +20% O_2) in response to increased heating rate. The Activation energies of maize cob and bean straw are 202.26 and 165.64 kJ mol^{-1} respectively.

Heating rate	Maize cob		Bean straw	
	n	A ($min^{-1}x10^{17}$)	n	A ($min^{-1}x10^{14}$)
10	10.0	8.14	9.3	3.00
20	10.1	7.20	9.0	2.73
30	10.2	7.02	9.3	3.27
40	10.3	6.66	9.4	3.38

Table 5
Reaction order (n) and pre-exponential factor (A) following pyrolysis in an inert environment (He) in response to increased heating rate. The activation energies of maize cob and bean straw are 214.15 and 252.09 kJ mol^{-1} respectively.

Heating rate	Maize cob		Bean straw	
	n	A ($min^{-1} \times 10^{18}$)	n	A ($min^{-1} \times 10^{23}$)
10	6.8	4.83	13.3	3.04
20	6.4	1.83	12.8	2.31
30	6.3	1.09	12.8	1.99
40	6.3	1.02	12.5	2.37

vs 1.5% [2]) since the resistance to thermal decomposition is in the order: hemicellulose < cellulose < lignin.

Pyrolysis and combustion of bean straw and maize cob can be described by a kinetic function of the form $(1-\alpha)^n$ where n is the order of reaction which ranged from 9.0 to 10.3 and 6.3–13.3 for both feedstocks in air and He respectively (Tables 4 and 5). The n values are relatively constant which suggests that the reaction mechanism is likely independent of heating rate. The order of reaction in this study is comparable to values reported for the pyrolysis of the microalgae *Chlorella vulgaris* (n = 9) [23] and soybean (n = 8.19–17.31) [42].

4. Conclusion

The combustion and pyrolysis of maize cob and bean straw in a thermogravimetric analyser occurred through moisture release, devolatilisation and char degradation. The produced gas during both pyrolysis and combustion contained H_2O, CO and CO_2 and their yields as well as the rate of feedstock degradation increased with increasing heating rate. Maize cob and bean straw have high volatile content, making them suitable feedstocks for thermochemical conversion methods. The activation energy in air was lower than in He which indicates that combustion is easier than pyrolysis from a reactivity viewpoint. Activation energy changed with conversion which indicates that the combustion and pyrolysis processes involve multiple reactions. Combustion and pyrolysis kinetic models were obtained, and the model can be used in predicting the combustion and pyrolysis behaviour of bean straw and maize cob.

Author contribution statement

David K. Okot: Conceived and designed the experiments; Performed the experiments; Analyzed and interpreted the data; Wrote the paper. Paul E. Bilsborrow, Anh N Phan, David A.C Manning: Contributed reagents, materials, analysis tools or data; Wrote the paper.

Data availability statement

Data will be made available on request.

Declaration of competing interest

The authors declare that they have no known competing financial interests or personal relationships that could have appeared to influence the work reported in this paper.

Acknowledgements

The authors would like to express their sincere gratitude to the UK Commonwealth Scholarship Commission for financial support and to Barfoots of Botley Ltd, UK for providing maize cobs used in this study.

References

[1] D.K. Okot, P.E. Bilsborrow, A.N. Phan, Thermo-chemical behaviour of maize cob and bean straw briquettes, Energy Convers. Manag. X. 16 (2022), 100313.
[2] D.K. Okot, P.E. Bilsborrow, A.N. Phan, Briquetting characteristics of bean straw-maize cob blend, Biomass Bioenergy 126 (2019) 150–158.
[3] M.A. Nadeem, M.Z. Yeken, M.Q. Shahid, E. Habyarimana, H. Yilmaz, A. Alsaleh, R. Hatipoglu, Y. Çilesiz, K.M. Khawar, N. Ludidi, S. Ercisli, M. Aasim, T. Karakoy, F.S. Baloch, Common bean as a potential crop for future food security: an overview of past, current and future contributions in genomics, transcriptomics, transgenics and proteomics, Biotechnol. Biotechnol. Equip. 35 (2021) 759–787.
[4] S. Maitra, T. Shankar, P. Banerjee, in: A. Hossain (Ed.), Potential and Advantages of Maize-Legume Intercropping System, Maize - Prod. Use, IntechOpen, 2020.
[5] T. Abbas, M. Issa, A. Ilinca, Biomass cogeneration technologies: a review, J. Sustain. Bioenergy Syst. 10 (2020) 1–15.
[6] M. Jahirul, M. Rasul, A. Chowdhury, N. Ashwath, Biofuels production through biomass pyrolysis —a technological review, Energies 5 (2012) 4952–5001.
[7] S. Yorgun, D. Yildiz, Slow pyrolysis of paulownia wood: effects of pyrolysis parameters on product yields and bio-oil characterization, J. Anal. Appl. Pyrolysis 114 (2015) 68–78.
[8] A. Mlonka-Medrala, P. Evangelopoulos, M. Sieradzka, M. Zajemska, A. Magdziarz, Pyrolysis of agricultural waste biomass towards production of gas fuel and high-quality char: experimental and numerical investigations, Fuel 296 (2021), 120611.
[9] S. Wang, H. Lin, B. Ru, G. Dai, X. Wang, G. Xiao, Z. Luo, Kinetic modeling of biomass components pyrolysis using a sequential and coupling method, Fuel 185 (2016) 763–771.
[10] P. Basu, Biomass Gasification, Pyrolysis, and Torrefaction: Practical Design and Theory, second ed., Academic Press is and Imprint of Elsevier, Amsterdam ; Boston, 2013.
[11] K. Slopiecka, P. Bartocci, F. Fantozzi, Thermogravimetric analysis and kinetic study of poplar wood pyrolysis, Appl. Energy 97 (2012) 491–497.
[12] M.Y. Guida, H. Bouaik, L. El Mouden, A. Moubarik, Utilization of Starink approach and avrami theory to evaluate the kinetic parameters of the pyrolysis of olive mill solid waste and olive mill wastewater, J. Adv. Chem. Eng. 7 (2017).
[13] C. Gai, Y. Zhang, W.-T. Chen, P. Zhang, Y. Dong, Thermogravimetric and kinetic analysis of thermal decomposition characteristics of low-lipid microalgae, Bioresour. Technol. 150 (2013) 139–148.
[14] T. Damartzis, D. Vamvuka, S. Sfakiotakis, A. Zabaniotou, Thermal degradation studies and kinetic modeling of cardoon (Cynara cardunculus) pyrolysis using thermogravimetric analysis (TGA), Bioresour. Technol. 102 (2011) 6230–6238.
[15] M.S. Ahmad, M.A. Mehmood, O.S. Al Ayed, G. Ye, H. Luo, M. Ibrahim, U. Rashid, I. Arbi Nehdi, G. Qadir, Kinetic analyses and pyrolytic behavior of Para grass (Urochloa mutica) for its bioenergy potential, Bioresour. Technol. 224 (2017) 708–713.
[16] Y. Liang, B. Cheng, Y. Si, D. Cao, H. Jiang, G. Han, X. Liu, Thermal decomposition kinetics and characteristics of Spartina alterniflora via thermogravimetric analysis, Renew. Energy 68 (2014) 111–117.
[17] C. Setter, F.T.M. Silva, M.R. Assis, C.H. Ataide, P.F. Trugilho, T.J.P. Oliveira, Slow pyrolysis of coffee husk briquettes: characterization of the solid and liquid fractions, Fuel 261 (2020), 116420.
[18] M. Poletto, A.J. Zattera, R.M.C. Santana, Thermal decomposition of wood: kinetics and degradation mechanisms, Bioresour. Technol. 126 (2012) 7–12.
[19] S.S. Idris, N.A. Rahman, K. Ismail, Combustion characteristics of Malaysian oil palm biomass, sub-bituminous coal and their respective blends via thermogravimetric analysis (TGA), Bioresour. Technol. 123 (2012) 581–591.
[20] S. Paniagua, S. Reyes, F. Lima, N. Pilipenko, L.F. Calvo, Combustion of avocado crop residues: effect of crop variety and nature of nutrients, Fuel 291 (2021), 119660.
[21] J. Liu, X. Jiang, H. Cai, F. Gao, Study of combustion characteristics and kinetics of agriculture briquette using thermogravimetric analysis, ACS Omega 6 (2021) 15827–15833.
[22] B.B. Nyakuma, Thermogravimetric and kinetic analysis of melon (Citrullus colocynthis L.) seed husk using the distributed activation energy model, Environ. Clim. Technol. 15 (2015) 77–89.
[23] C. Chen, X. Ma, Y. He, Co-pyrolysis characteristics of microalgae Chlorella vulgaris and coal through TGA, Bioresour. Technol. 117 (2012) 264–273.
[24] S.A. El-Sayed, M. Khairy, Effect of heating rate on the chemical kinetics of different biomass pyrolysis materials, Biofuels 6 (2015) 157–170.
[25] Z. Boubacar Laouge, H. Merdun, Pyrolysis and combustion kinetics of Sida cordifolia L. using thermogravimetric analysis, Bioresour. Technol. 299 (2020), 122602.
[26] G.K. Gupta, M.K. Mondal, Kinetics and thermodynamic analysis of maize cob pyrolysis for its bioenergy potential using thermogravimetric analyzer, J. Therm. Anal. Calorim. 137 (2019) 1431–1441.
[27] E.A. Castiblanco, J.H. Montoya, G.V. Rincon, Z. Zapata-Benabithe, R. Gomez-Vasquez, D.A. Camargo-Trillos, A new approach to obtain kinetic parameters of corn cob pyrolysis catalyzed with CaO and $CaCO_3$, Heliyon 8 (2022), e10195.
[28] R. Lopez, C. Fernandez, J. Fierro, J. Cara, O. Martinez, M.E. Sanchez, Oxy-combustion of corn, sunflower, rape and microalgae bioresidues and their blends from the perspective of thermogravimetric analysis, Energy 74 (2014) 845–854.
[29] A. Agrawal, S. Chakraborty, A kinetic study of pyrolysis and combustion of microalgae Chlorella vulgaris using thermo-gravimetric analysis, Bioresour. Technol. 128 (2013) 72–80.
[30] I. Boumanchar, Y. Chhiti, F.E. Mhamdi Alaoui, M. Elkhouakhi, A. Sahibed-dine, F. Bentiss, C. Jama, M. Bensitel, Investigation of (co)-combustion kinetics of biomass, coal and municipal solid wastes, Waste Manag. 97 (2019) 10–18.
[31] F. Nocera, A. Gagliano, F. Patania, M. Bruno, S. Scire, Slow pyrolysis kinetics of apricots stones by Thermogravimetric Analysis, in: 2016 7th International Renewable Energy Congress IREC, IEEE, Hammamet, Tunisia, 2016, pp. 1–6.
[32] L. Zhang, C. (Charles) Xu, P. Champagne, Overview of recent advances in thermo-chemical conversion of biomass, Energy Convers. Manag. 51 (2010) 969–982.
[33] N.T. Farrokh, H. Suopajarvi, P. Sulasalmi, T. Fabritius, A thermogravimetric analysis of lignin char combustion, Energy Proc. 158 (2019) 1241–1248.
[34] T. Mani, P. Murugan, J. Abedi, N. Mahinpey, Pyrolysis of wheat straw in a thermogravimetric analyzer: effect of particle size and heating rate on devolatilization and estimation of global kinetics, Chem. Eng. Res. Des. 88 (2010) 952–958.

[35] M. Radojević, B. Janković, V. Jovanović, D. Stojiljković, N. Manić, Comparative pyrolysis kinetics of various biomasses based on model-free and DAEM approaches improved with numerical optimization procedure, PLoS One 13 (2018) 1–25.
[36] D. Li, L. Chen, S. Chen, X. Zhang, F. Chen, N. Ye, Comparative evaluation of the pyrolytic and kinetic characteristics of a macroalga (Sargassum thunbergii) and a freshwater plant (Potamogeton crispus), Fuel 96 (2012) 185–191.
[37] F.-X. Collard, J. Blin, A review on pyrolysis of biomass constituents: mechanisms and composition of the products obtained from the conversion of cellulose, hemicelluloses and lignin, Renew. Sustain. Energy Rev. 38 (2014) 594–608.
[38] D. Vamvuka, S. Sfakiotakis, Combustion behaviour of biomass fuels and their blends with lignite, Thermochim. Acta 526 (2011) 192–199.
[39] P. Ninduangdee, V.I. Kuprianov, E.Y. Cha, R. Kaewrath, P. Youngyuen, W. Atthawethworawuth, Thermogravimetric studies of oil palm empty fruit bunch and palm kernel shell: TG/DTG analysis and modeling, Energy Proc. 79 (2015) 453–458.
[40] D. Lopez-Gonzalez, M. Fernandez-Lopez, J.L. Valverde, L. Sanchez-Silva, Kinetic analysis and thermal characterization of the microalgae combustion process by thermal analysis coupled to mass spectrometry, Appl. Energy 114 (2014) 227–237.
[41] S. Hu, X. Ma, Y. Lin, Z. Yu, S. Fang, Thermogravimetric analysis of the co-combustion of paper mill sludge and municipal solid waste, Energy Convers. Manag. 99 (2015) 112–118.
[42] X. Huang, J.-P. Cao, X.-Y. Zhao, J.-X. Wang, X. Fan, Y.-P. Zhao, X.-Y. Wei, Pyrolysis kinetics of soybean straw using thermogravimetric analysis, Fuel 169 (2016) 93–98.
[43] P. Sittisun, N. Tippayawong, D. Wattanasiriwech, Thermal degradation characteristics and kinetics of oxy combustion of corn residues, Adv. Mater. Sci. Eng. (2015) 1–8.
[44] W. Wu, Y. Mei, L. Zhang, R. Liu, J. Cai, Kinetics and reaction chemistry of pyrolysis and combustion of tobacco waste, Fuel 156 (2015) 71–80.
[45] I. Obernberger, G. Thek, Physical characterisation and chemical composition of densified biomass fuels with regard to their combustion behaviour, Biomass Bioenergy 27 (2004) 653–669.